Phonon dispersion curves and elastic properties of polyoxymethylene single crystals

M. R. Anderson*, M. B. M. Harryman, D. K. Steinman*** and J. W. White†**

Physical Chemistry Laboratory, Oxford University, South Parks Road, Oxford OX1 3QZ, UK

and R. Currat

Institut Laue-Langevin, 156X, 38042 Grenoble, France

(*Received* 29 *June* 1981)

By growing large single crystals of fully deuterated polyoxymethylene $(CD_2O)_n$, it has been possible to observe phonons for a number of different branches of the phonon dispersion curves using coherent neutron inelastic scattering. Using a hexagonal approximation for this crystal, four of the five independent stiffness constants at 300K have been determined as $C_{11}=1.30\times10^{11}$; $C_{12}=6.32\times10^{10}$; $C_{33}=1.64\times10^{12}$; $C_{44}=2.64\times10^{10}$ dyne cm^{-2} from the acoustic slopes. The hexagonal approximation is valid to within 10% and this is discussed. The inherent disorder and large size of the unit cell along the *c* axis (17.35 Å) have restricted modelling of the lattice dynamics by methods such as the atom–atom potential method, and made phonon measurements impracticable in some regions of the momentum transfer–energy transfer space.

Keywords Crystals; elasticity; phonon dispersion curves; polyoxymethylene

INTRODUCTION

The characteristic molecular disorder which prevails in high polymer solids gives them their unique physical properties. In particular, the elasticity of bulk specimens can only be understood by supposing that the materials have a composite texture. In this model, crystalline blocks hundreds of angstroms on edge, and containing close-packed molecular chains, are assumed to be joined together by amorphous material where the same chains are tangled and disordered[1,2]. The crystalline regions are in most respects similar to simple molecular crystals and generally have anisotropic elastic properties. The elasticity of the amorphous materials is assumed to be isotropic. By taking Voigt or Reuss averages[3] over the two regions, it is then possible to model the bulk elastic properties.

Neither the composite model nor the averaging procedures have been tested fully because experimental values for the stiffness matrix of the crystals and the amorphous modulus are lacking. Even the elegant method of Sakurada and his school[4] for measuring truly crystalline elastic strains in polymers by X-ray diffraction is limited by uncertainty in the homogeneity of the stress and strain fields. Only for polyethylene[5] has an attempt been made to discuss polymer elasticity at the microscopic level of the intra- and intermolecular forces.

† Author to whom correspondence should be sent

Present addresses:

* Materials Physics Division, AERE, Harwell, Didcot, Oxon, UK

** Department of Environment, London, UK

*** I.R.T. Corporation, San Diego, California, USA

Measurements of the phonon dispersion curves for polymers by inelastic neutron scattering spectroscopy in principle allow the crystalline stiffness constants to be determined and can test microscopic force field models[5]. With stretched samples, chain axis phonons have been observed in polyethylene and polytetrafluoroethylene[6-9], while annealing under pressure has produced samples of deutero-polyethylene in which longitudinal excitations were detected along the $\zeta00$ and $\zeta\zeta0$ and $0\zeta0$ directions perpendicular to the chain axis[10]. Some dispersion curves for modes perpendicular to the chain axis have been measured even for polycrystals[11,12] but all of these experiments have yielded largely elastic constants for longitudinal acoustic waves. Measurements of transverse acoustic waves, and hence shear stiffnesses, have not been possible generally for the lack of large single crystal specimens.

In this paper we report the preparation of large specimens of protonated and deuterated polyoxymethylene with single crystal texture and their use for three dimensional phonon dispersion curve measurements.

Crystal structure

Polyoxymethylene (POM) is a polymer of formaldehyde, and two crystalline forms, hexagonal and orthorhombic, are stable at room temperature. The hexagonal form consists of helical chains of the monomer $(-CH_2O-)$ close packed to give lattice parameters $c=17.35$ Å, $a=4.46$ Å and one 'chain' per unit cell. The unit cell has five turns of the helical molecule containing, in all, nine monomer units (a 9/5 helix)[13-15] and

0032-3861/82/040569-09$03.00

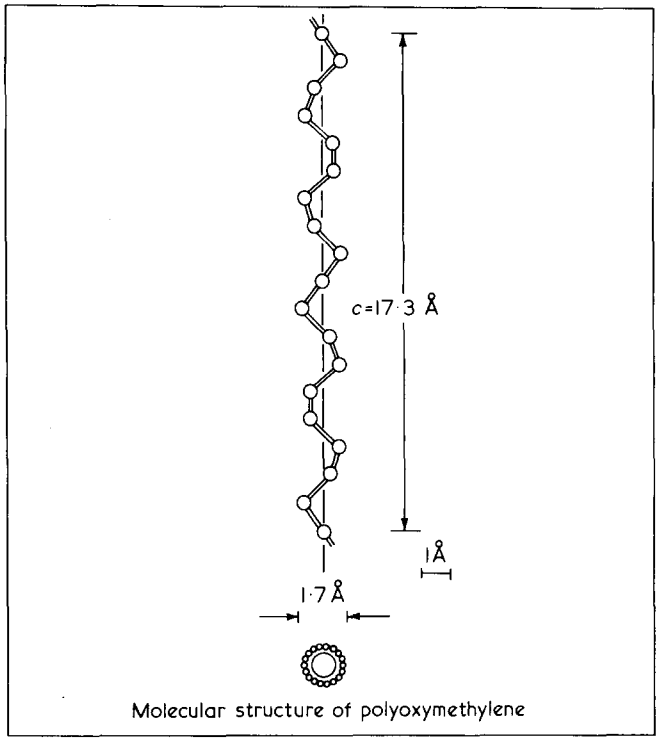

Figure 1 Arrangement of the chain in the unit cell of hexagonal polyoxymethylene (from Uchida and Tadokoro[13])

dispersion forces between oxygen and CH_2 groups stabilize the *gauche* conformations which generate the helix[16]. However a recent X-ray study of very small single crystals of hexagonal polyoxymethylene obtained by growth from sulphuric acid–water solution gives somewhat different lattice parameters[17]. Gramlick proposes P2 space group, helix uncertain but 2*38/21 assumed, with reference basis orthohexagonal $a=4.469$ Å, $b=7.740$ Å, $c=73.4$ Å. From 896 reflections $R=0.042$ was obtained.

The trigonal space group for POM from trioxane is C_3^1 or C_3^2,[13] which are appropriate to a left-handed and right-handed helix respectively. The handedness of the helix is not distinguishable if the crystal contains only one type[13] but, as yet, a decisive crystallographic study with neutrons has to be done. *Figure 1* (from ref. 13) shows the arrangement of the chain, and *Table 1* contains the structural data for the hexagonal POM sample used as measured with neutrons. The positions of all 36 atoms in the unit cell can be obtained from the cylindrical coordinates of the four atoms in a monomer by performing a rotation through $n2\pi/9$ and a translation along the c-axis of $nc/9$ for each other monomer ($n=1$–9) in the primitive cell.

Lattice dynamics

The 36 atoms in the unit cell give rise to 108 branches in the phonon dispersion relations and the length of the c axis chain repeat (17.35 Å) leads to a very small half Brillouin zone (0.1811 $Å^{-1}$) which complicates phonon measurements with conventional triple axis neutron spectrometers. Because of the large cell size, a complete lattice dynamics calculation has not yet been attempted. In the basal plane, phonon branches were sought near the few intense Bragg reflections. For the c-axis excitations, inelastic structure factors were calculated from eigenvectors for a single chain model (SCM) by Piseri and Zerbi[18] to guide the measurements. Because of the short range of the valence forces in the chain, it is convenient to represent the c-axis lattice dynamics in an extended zone based on the projection of the molecular repeat unit rather than the unit cell.

A qualitative understanding of the consequences of this can be seen from the standard equations of motion. For the displacement from equilibrium, $u(sld)$, of the $d$the atom of the sth CH_2O group in the lth unit cell in the direction α:

$$m_{sd}\ddot{U}_\alpha(lsd) = -\sum_{ls'd'\beta} F_{\alpha\beta}\begin{pmatrix} l's'd' \\ l\,s\,d \end{pmatrix} U_\beta(l's'd') \qquad (1)$$

where m_{sd} is the mass of the (sd)th atom (and hence the index s may be dropped), and $F_{\alpha\beta}\begin{pmatrix} l's'd' \\ l\,s\,d \end{pmatrix}$ is the force constant between atoms $(l's'd')$ and (lsd). Using the standard solution,

$$U_\alpha(lsd) = \frac{e_\alpha(sdq)}{m_d^{1/2}} e^{i(q.\underset{\sim}{X}(l)+\omega t)}$$

where $\underset{\sim}{X}(l)$ is a vector to the origin of the lth unit cell, results in the equation

$$\omega^2 e_\alpha(sdq) = \sum_{s'd'\beta}\left\{(m_d m_{d'})^{-1/2}\sum_{l'} F_{\alpha\beta}\begin{pmatrix} l's'd' \\ l\,s\,d \end{pmatrix} e^{-iq[\underset{\sim}{X}(l')-\underset{\sim}{X}(l)]} e_\beta(d')\right. \qquad (2)$$

The quantity in the brackets of equation (2), the dynamical matrix, $D_{\alpha\beta}\left(\begin{matrix} s\,d \\ s'd' \end{matrix}\middle| q\right)$, represents a set of $3np$ (n=number of atoms per chemical repeat unit; p=number of repeat units per primitive unit cell) equations in the eigenvalues, $\omega^2(q)$, and eigenvectors $e(sdq)$, there being $3nm$ values of $\omega^2(q)$ for each value of q, the wave bector, within the first Brillouin zone. The eigenvalues $\omega^2(q)$, are the roots of the secular equation

$$|\underset{\sim}{D}(q) - \omega^2 I| = 0 \qquad (3)$$

In the z direction the Brillouin zone boundary is at $\frac{\pi}{c}$. The SCM is introduced in order to reduce the dimensionality of equations (2) and (3), and it consists of the following restrictions and approximations[18]:

(1) $\underset{\sim}{q}$ is parallel to $\underset{\sim}{z}$, i.e. only collective motions propagating in the chain direction are considered.

Table 1 Crystal structure data for hexagonal polyoxymethylene

Material and conditions	c (Å)	a (Å)	Comments
^{1}H Polyoxymethylene (300K)	17.37	4.57	DIDO MK6 (Harwell)
^{2}D Polyoxymethylene (300K)	17.35	4.48*	IN2 (I.L.L.)
	17.35	4.56	DIDO MK6 (Harwell)
(120K)	17.35	4.42	IN2 (I.L.L.)

* We believe that this discrepancy is due to the difficulty of making measurements on the large, highly-attenuating crystal

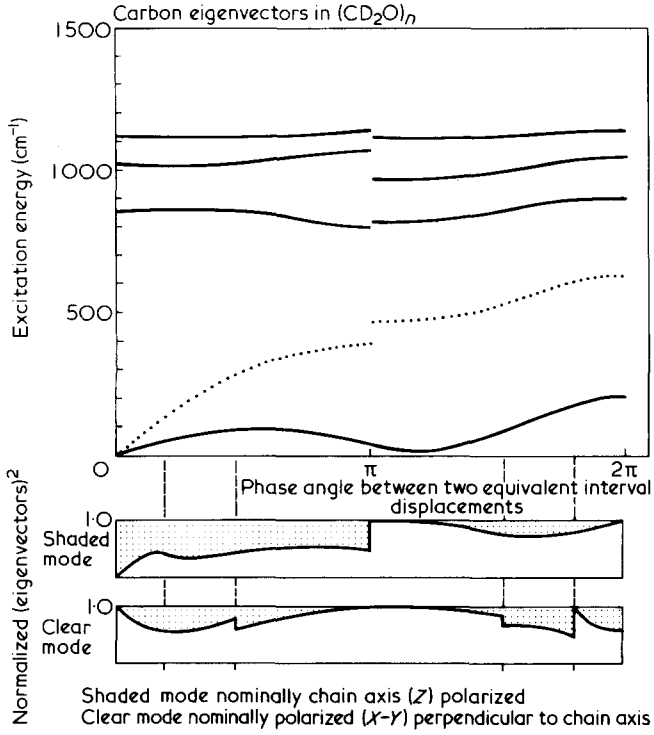

Figure 2 Deuteron (mode eigenvectors)^2 for nominal longitudinal acoustic (a) and transverse acoustic (b) phonons propagating along the polymer chain direction

(2) The forces acting between atoms in the same chain are much greater than those acting between atoms on different chains. The interchain forces are set equal to zero.

(3) The normal mode displacements of equivalent atoms in different chemical units within the cell are related by the expression

$$e(s'd) = e(sd)e^{-iq.[X(s')-X(s)]} \tag{4}$$

and substituting equation (4) into equation (2) and letting $s = l = 0$ gives:

$$\omega^2 e(d) = \sum_{d'\beta}\left\{(m_d m_{d'})^{-1/2}\sum_{l's'} F_{\alpha\beta}\begin{pmatrix} l's'd' \\ l\,s\,d \end{pmatrix} e^{-iq.[X(l's')-X(ls)]}\right\} e_\beta(d') \tag{5}$$

Equation (5) and its associated secular equations represent a system of only $3n$ equations for the eigenvalues and eigenvectors. It appears that $3n(p-1)$ solutions have been discarded but it must be noted that equation (5) no longer has the periodicity of $\frac{\pi}{c}$ but of $\frac{9\pi}{c}$. Hence q must be extended by a factor of nine and the missing solutions are recovered. It is important to note from equation (2) that the set of eigenvectors, $e(sd|q)$, generated from the $e(d|q)$ by applying equation (4) for the $p-1$ values of s in the primitive cell still retain the periodicity of $\frac{\pi}{c}$.

Such an extended zone representation is convenient as it folds out the many branches which necessarily arise from the small (π/c) Brillouin zone. The deficiencies of the representation appear when the mode eigenvectors are examined across the extended zone. *Figure 2* shows a graph of (carbon eigenvectors)^2 for the nominal longitudinal acoustic and transverse acoustic modes in the chain direction. It is clear that the nominal polarizations (LA and TA) describe the vibrations correctly only at low q values within the small $\left(\frac{\pi}{c}\right)$ zone. The polarization of either mode rapidly becomes about 1/3 of the nominal as the first true *b.z.b.* is approached and there are strong variations in polarization near the zone centres and boundaries at higher q (i.e. at $\frac{\pi}{c}$, $\frac{2\pi}{c}$ etc.) This periodicity appears also in the behaviour of the elastic structure factors in hydrogenous POM. The effect is shown in *Figure 3a* and *b* where experimental values of F^2_{hkl} are plotted against l for several h and k values. This is part of the pattern of layer lines expected in diffraction from helical structures[19]. Since the inelastic scattering intensities of acoustic modes are strongly correlated with the elastic scattering intensities from the reciprocal lattice point, they also vary rapidly in the c direction. The same general conclusion holds for the deuterated polymer, but some reciprocal lattice points have very different intensities due to the difference of scattering length between H and D (see Experimental section).

For the deuterated crystal, inelastic structure factors were computed from Piseri and Zerbi's SCM eigenvectors by using the extended zone representation but choosing the true reciprocal lattice points as origins for the extended zones. The use of such structure factors is limited because the complexity of the eigenvectors and of the positions of atoms within the unit cell combine to yield almost random phases. Only where the eigenvectors had

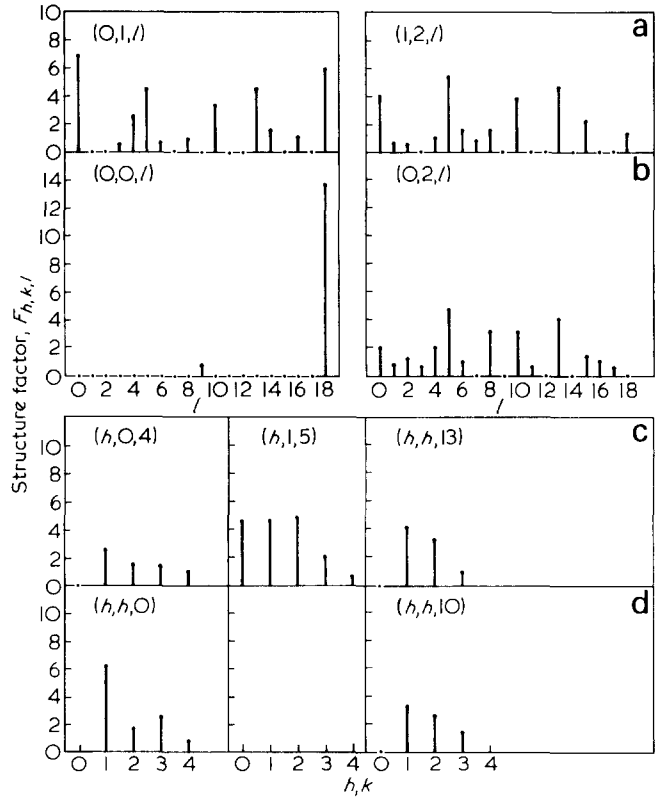

Figure 3 (a) and (b) Variation of the elastic scattering structure factor, F_{hkl} as a function of l for several h and k values
(c) and (d) Variation of the elastic scattering structure factor, F_{hkl} as a function of h, k for given l values

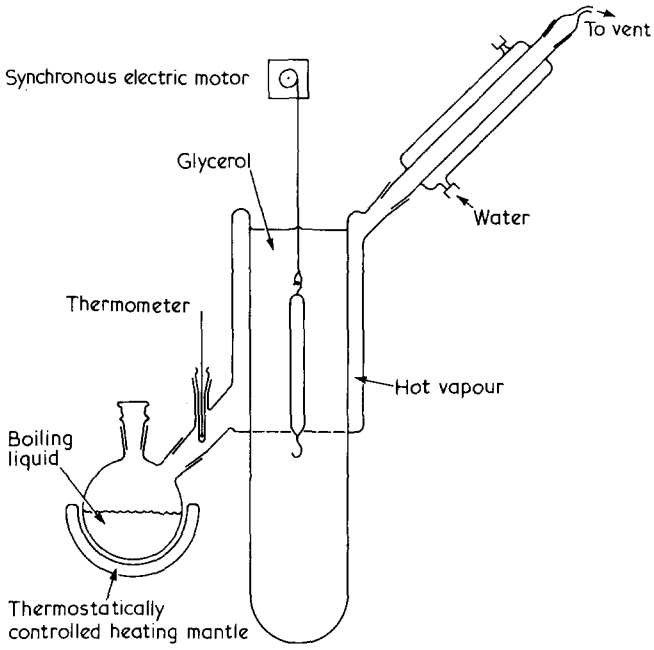

Figure 4 Modified Bridgman apparatus for growing trioxane crystals

obvious polarizations did the structure factors aid the observation of phonons.

By contrast with the c direction, the elastic structure factors as a function of h, k at various l levels vary smoothly and the results for hydrogen polyoxymethylene crystals are shown in *Figure 3c* and *d*.

EXPERIMENTAL

Preparation of the polymer 'single' crystal

Polyoxymethylene may be produced by radiation polymerization[13-15,20] of trioxane (TOX) or tetroxane (TOM), the cyclic trimers and tetramers of formaldehyde respectively. The polymerization is topotactic and the resulting crystals of polymer have three-dimensional order with axes in a defined relationship to the precursor crystal axes. There are a number of important morphological differences between polymers from the two sources, in particular the tetroxane samples give strong meridional, low angle, X-ray diffraction peaks due to chain folds which may be up to 250 Å apart depending upon the preparative method[20].

TOM is a better precursor for POM than is TOX for several reasons. The fraction of TOM converted is usually 98–100%, whereas TOX has a conversion of the order of 75%. Since the yield is higher for TOM, the density of the POM is also higher. The most important consideration from the standpoint of diffraction experiments is that POM from a single crystal of TOM is itself a single crystal, but the POM from a single TOX crystal is composed of fibrous crystal bundles with some twinning in each fibril (see below). Due to difficulties in producing single crystals and the unavailability of deuterated tetroxane, the POM sample used in the present study was obtained from trioxane with annealing to remove twinned components[20-22].

Deuterated trioxane mixed with D_2O was prepared by fractional distillation at 94°C of a constant boiling mixture of deuterated *para*-formaldehyde, D_2O and D_2SO_4 over a period of severl hours. The trioxane was then extracted into methylene chloride which was dried over $CaCl_2$ and evaporated at 0°C. It was important not to allow the trioxane to become too dry otherwise spontaneous polymerization occurred. The *para*-formaldehyde was supplied by Merck, Sharpe and Dohme Ltd. of Canada and the deuteration was quoted as better than 98%.

The deuterotrioxane, DTOX, was grown into a single crystal in a Bridgman apparatus adapted to anneal the crystal through its plastic phase to room temperature. This was the only successful method of the many that were tried. The apparatus is shown in *Figure 4* and consists of a tube filled with glycerol, the upper part vapour jacketed and the lower part at room temperature. The temperature gradient at the interface between the hot and cold parts was about 40°C cm^{-1} and the upper temperature was just above the melting point of the DTOX as prepared (~59°C). The tube containing the DTOX was lowered through the gradient at about 1.2 cm per day or less. This procedure also refined the DTOX forcing impurities to remain on the liquid side of the gradient. Parts of the DTOX crystal spontaneously polymerized to DPOM. The DTOX crystal was irradiated with 0.5 Mrad of ^{60}Co γ-rays and placed overnight in an oven at 45°C to encourage polymerization. The temperature was then raised to 57°C for several hours and afterwards to 90°C to drive the unpolymerized DTOX out of the DPOM crystal. The DPOM crystal had a density of 1.0 as compared with the theoretical density of 1.59 g cm^{-3} calculated from the lattice parameters. The material has a high lustre and an obviously fibrous texture. After heat treatment to reduce the twinning, the cylindrical sample (17 mm diameter × 30 mm) had a density of 0.8 and weighed 6.6 g.

Using the above procedure several large specimens of hydrogenous polyoxymethylene have been grown for X-ray and neutron diffraction as well as macroscopic mechanical testing. An example showing the size and uniformity of the polymer texture is shown viewed sideways and end on in *Figures 5* and *6*.

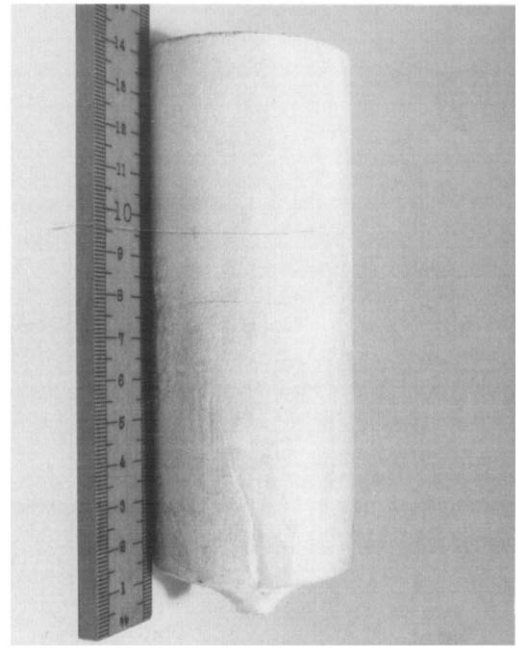

Figure 5 Large 'crystal' showing two grains after annealing at 170°C

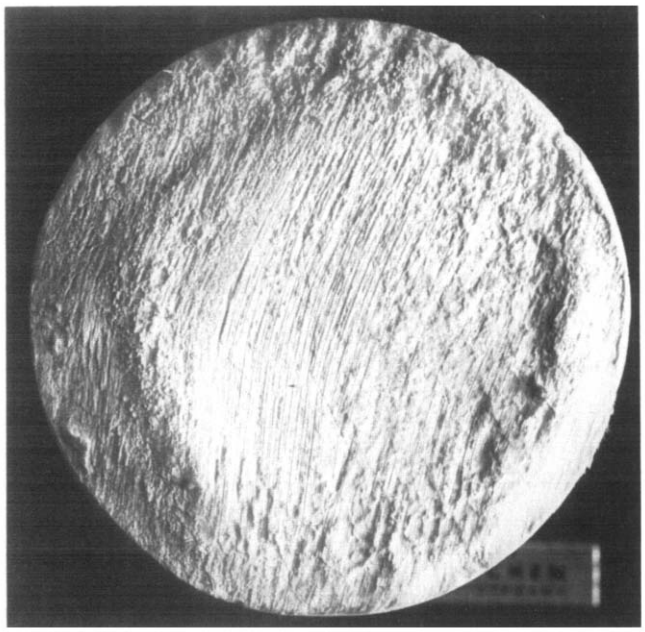

Figure 6 Top face of the same 'crystal' showing the emergence of the grain boundaries at the top growing surface

Neutron and X-ray diffraction

Neutron and X-ray diffraction patterns from normal and deuterated POM crystals were observed prior to and during the inelastic experiments to characterize the samples and to follow the annealing treatment used to remove twinning. A detailed study of the structure by neutron diffraction is in progress.

Twinning. Polyoxymethylene from TOX exhibits a form of homogeneous twinning[21,22] in which each fibril consists of a main or '*Z*' crystal whose '*c*' axis is parallel to the '*c*' axis of the TOX, and '*W*' crystals whose (100) axes coincide with those of the '*Z*' crystals but whose '*c*' axis makes an angle of 76° 7′ with the '*c*' axis of the '*Z*' crystal.

To detect the twinning, rotating crystal X-ray photographs of polymer fibre bundles with the *c*-axis vertical were taken. *Figure 7* shows diffraction from a 5 mm × 0.5 mm × 0.5 mm HPOM 'crystal' at two different exposures. The equator and the fifth layer lines can be clearly seen in *Figure 7a* as well as the four spots at 76° 7′ to the equator which arise from the twinned crystals. More of the layer lines and some interesting disorder appear in the longer exposure (*Figure 7b*) but both plates illustrate the very high degree of crystalline order obtained in typical specimens.

It has been found[22,23] that heating POM from TOX to 170°C for several hours removes most of the twinned material. The heating process results in both annealing and recrystallization of the '*W*' crystals into the '*Z*' orientation, as well as degradation of the POM of both orientations to monomer. The heat-treated material becomes very porous and loses mechanical strength. For this reason the DPOM sample was given only a mild heat treatment resulting in the 6.6 g crystal used in all diffraction and three-axis measurements reported below.

Neutron diffraction. Four-circle neutron diffraction experiments were performed on a piece of the 6.6 g deuterated crystal and on thin slices of the HPOM using the Mk VI diffractometer on the DIDO reactor at AERE, Harwell. Some of the data for HPOM are shown in *Figure 3a, b, c,* and *d.* Very pronounced changes of the scattered intensities were found on deuteration. *Table 2* compares the intensities of some important reflections uncorrected for sample geometry. The effect of isotopic substitution on the (0,0,18) is particularly noteworthy.

In each of the HPOM (or DPOM) crystals, a similar mosaic spread was observed. A rocking curve of any reciprocal lattice point taken by rotating the sample around the '*c*' axis gave a FWHM near 4°, but a rocking curve taken by rotating the crystal around any axis

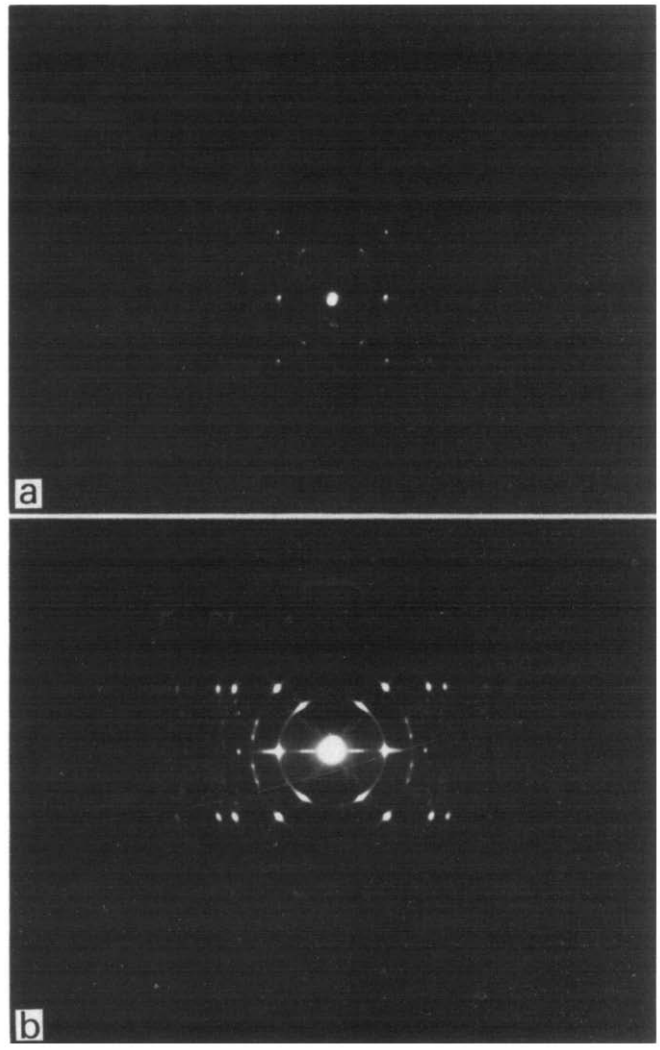

Figure 7 (a) Short exposure rotation photograph of a polyoxymethylene fibre bundle of single crystal habit with the polymer chain axis vertical. (b) Longer exposure for the same 'crystal' showing the fifth and higher layer lines as well as some disorder and the twinning

Table 2 Isotopic substitution effect on the scattered intensities from hydrogen and deuterium polyoxymethylene

Reflection	Hydrogen POM Relative intensity	Deuterium POM Relative intensity
(1,0,0)	151	123
(1,0,4)	18	52
(1,0,5)	50	47
(1,0,10)	18	3
(1,0,13)	27	3.4
(1,0,18)	48	16.6
(0,0,18)	239	3.8

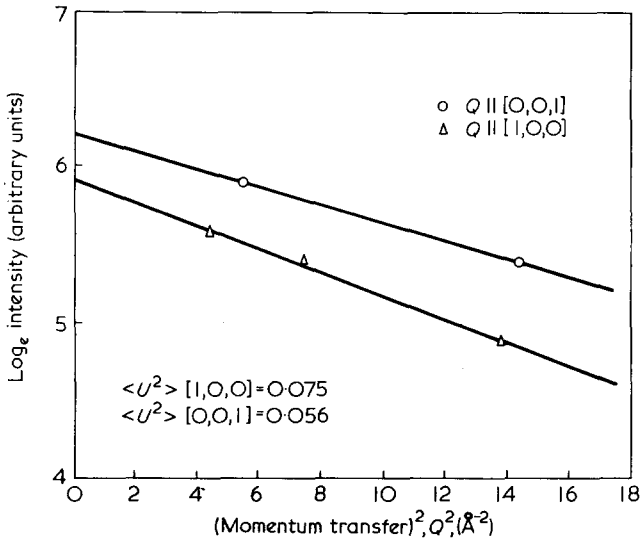

Figure 8 Debye–Waller factor analysis for mean thermal vibrational amplitudes along the c^* and a^* axes in deutero-polyoxymethylene

perpendicular to 'c' gave a FWHM of 0.5°. Thus the POM samples may be characterized as having excellent 'c' axis alignment, but adjacent helices or microfibrils show some rotational disorder.

Several unsuccessful attempts were made to observe reciprocal lattice points belonging to the twinned lattice in DPOM. The rotations needed to bring a twinned reciprocal lattice point into the reflecting position can be readily deduced from the X-ray results in the literature[13–15]. No detectable increase in scattering intensity was observed at any location in the reciprocal lattice obtained from these calculations, so it is concluded that the amount of twinning in the DPOM sample may not at present be measured by high angle elastic neutron scattering.

Measurements of the Debye–Waller factors for the momentum transfer, $Q\left(=\frac{4\pi}{\lambda}\sin\theta_B\right)$, parallel to the '$c$' and '$a$' axes, were made with triple-axis spectrometer at DIDO, AERE, Harwell. The scattering plane used for these measurements was the same as used for most of the phonon scans along the c^*–a^* plane (see next section). The positions of Bragg peaks along c^* and a^* were determined by θ–2θ scans along these axes. Then constant Q scans were made through $\Delta E = 0$ for several Q values placed so as to avoid the Bragg peaks, thereby sampling the incoherent scattering. Mean vibrational displacements of D atoms along 'c' (0.237 Å) and along 'a' (0.274 Å) were calculated from these measurements. The plot of natural log (elastic intensity) *versus* Q^2 is shown in *Figure 8*. The resolution-broadened FWHM of all the scans was the same.

PHONON MEASUREMENTS

Neutron spectrometers

Phonon groups were detected in the deutero-polyoxymethylene crystal using the IN2 and IN8 triple-axis spectrometers at the Institut Laue-Langevin, Grenoble, and that at the 10H beam hole of the DIDO reactor, AERE, Harwell.

The IN2 is a Steadman (double monochromator) instrument. The incident energy was kept constant and the final energy, E_f, varied. Two different sets of monochromator crystals were used. The high energy transfer scans were made using two matching Cu (111) crystals. Very good resolution was necessary to define the low energy $TA(001)$ mode unambiguously because of nearby Bragg peaks, so two matching pyrolytic graphite crystals were installed and the (002) planes used to select neutrons at $E_0 = 14.7$ meV. A pyrolytic graphite filter 5 cm long was used in conjunction with these monochromators and reduced the second order contamination of the incident beam so that the ratio of first to second order reflections from the monochromators was better than 100:1. In all cases on IN2 the analyser was pyrolytic graphite set to the (002) reflection.

The IN8 instrument is a conventional triple-axis spectrometer optimized for maximum flux on a thermal beam hole at ILL. Both monochromator and analyser were graphite (002) and a constant final energy of 14.7 meV was used in conjunction with a 5 cm pyrolytic graphite filter before the analyser.

The 10H triple-axis spectrometer at DIDO has several fixed take-off angles for selecting E_0. So all energy scans must vary E_f. Unfortunately, the fixed take-off angles do not coincide with the energy needed to use a pyrolytic graphite filter. Second order contamination was reduced by using a germanium (111) as analyser. *Figure 9* shows a moderately good transverse acoustic phonon group measured on IN2 and at the DIDO triple-axis machine. The excellent low background of IN2 is immediately obvious, making it possible to observe the weaker phonons along the c axis in DPOM.

Results

Phonons propagating along the c*-axis (IN2, DIDO 10H).* The crystal of DPOM was aligned with the (001) and (100) reciprocal lattice points in the scattering plane. The mosaic of the crystal in this orientation behaves so that any rocking curve in the scattering plane has the narrow width appropriate to the 'c' axis orientation. Alignment of the (100) in the scattering plane involves a rotation about the (001) axis whose large mosaic spread causes some uncertainty. The scattering 'points' may thus be thought of as thin bars through the reciprocal lattice and normal to the scattering plane. In such a situation relaxed vertical

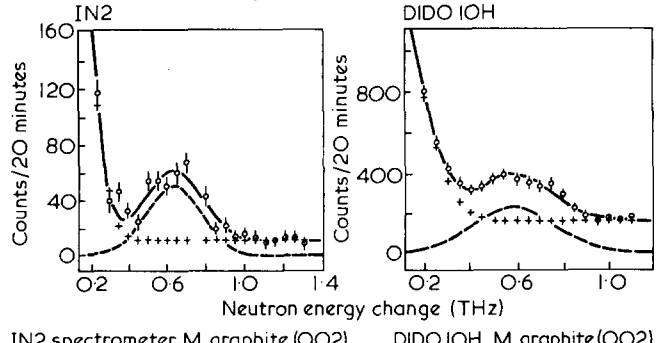

Figure 9 Comparison of the same $TA(001)$ phonon taken in a constant Q scan at (1, 0, 0.6) on the IN2 and DIDO 10H triple axis spectrometers. The neutron energy transfer is in terahertz (10^{12} s^{-1}), THz

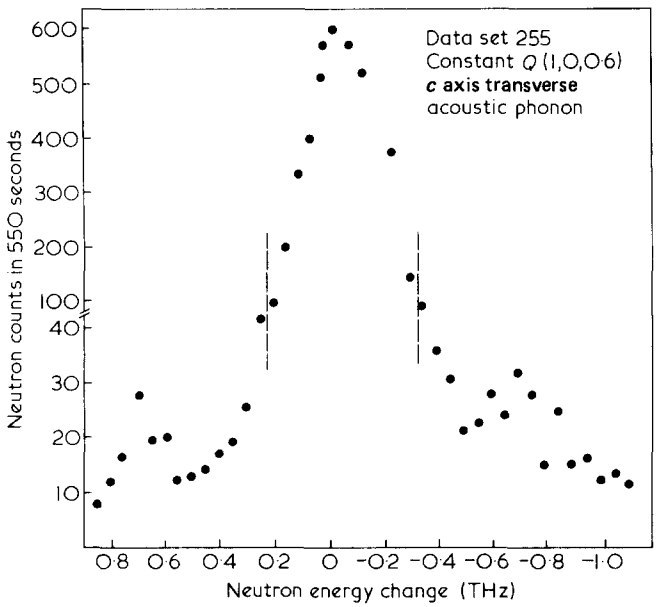

Figure 10 Neutron Brillouin triplet showing *c* axis transverse acoustic phonons in energy gain and energy loss for deutero-polyoxymethylene at 298K. The large central peak comes from the incoherent elastic scattering

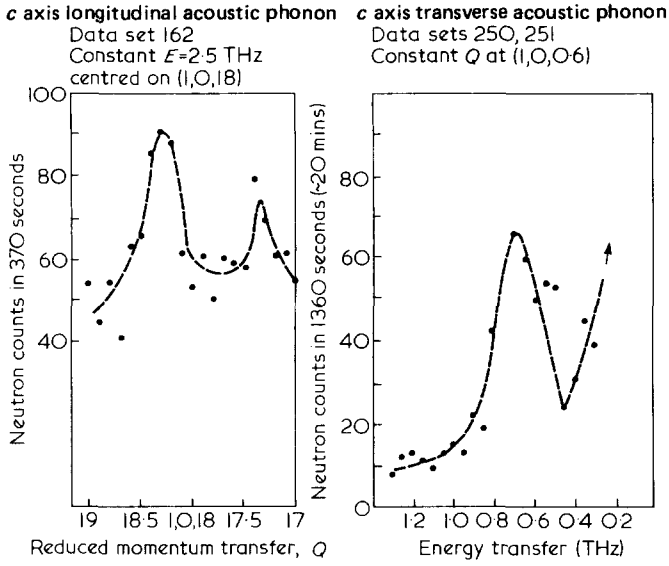

Figure 11 Longitudinal and transverse acoustic phonons along some crystal directions in deutero-polyoxymethylene

collimation is useful to enhance the phonon intensity. This produces only a slight error in phonon wavevectors for the mosaic widths of the sample used.

Based on the fact that the intensity of acoustic phonons near $q=0$ is proportional to the elastic structure factor, both the *TA* (001) and *LA* (100) were sought near (1,0,0), the most intense reciprocal lattice point in the crystal. The former was observed with difficulty but the latter was not seen.

Figure 10 shows the first observation of transverse acoustic phonons in a polymer and gives the full Brillouin triplet. The energy gain and energy loss peaks have different widths because of neutron focusing. The weakness of both the neutron energy gain and energy loss phonons, compared to the incoherent elastic peak, illustrates some of the experimental difficulties raised by this material. This particular phonon was difficult to observe since the whole branch is at low frequency. The Q range available for measurements is restricted at the one end by the shortness of the Brillouin zone, and at the other end because incoherent elastic scattering from the deuterium atoms causes the intensity of the phonon peak to be masked near $q=0$. The tail of the resolution function passing through the (1,0,0) also masks the peak. To identify this phonon branch definitively it was necessary to use a well-filtered beam from graphite (alternatively, to use the Ge (111) as an analyser) at low incident energy (for improved resolution), and to look on both sides of $E=0$, i.e. focused and defocused scans. Once identified, the branch could only be followed to $0.9\left(\frac{2\pi}{c}\right)$ as its structure factor decreased rapidly across the Brillouin zone. Representative phonons from IN2 for this branch, and for the *c*-axis longitudinal acoustic mode *LA* (001), are shown in *Figure 11*. All measured phonons were fitted to a Gaussian shape with either linear or Gaussian background functions by means of a least squares fitting code obtained from Dr H. G. Smith at the Solid State Division of Oak Ridge National Laboratory. This code is especially useful to obtain energies, amplitudes and resolution widths for each phonon, such as those in *Figure 9*, where the peak of interest occurs in the wings of a much more intense peak.

The principal criteria used to choose spectrometer scans were the inelastic structure factors from Zerbi's single chain model calculations (particularly for the (001) branches) and the elastic structure factors.

Figure 12 shows the range of (q,ω) space explored in the above experiments, superimposed on Zerbi's deuteropolyoxymethylene single chain model calculations. The extended zone representation is used. The *LA*(001) was followed to $0.9\left(\frac{2\pi}{c}\right)$ by making constant E scans away from the (1,0,18) reciprocal lattice point. *Figure 12* also shows that, beyond $0.9\left(\frac{2\pi}{c}\right)$, a cross-over region with the optic branch is expected, and indeed the phonons became too weak to be clearly observable around the (1,0,19) or (1,0,17). Although scans were attempted at other reciprocal lattice points, no definite further observations of this branch were made. Attempts to locate

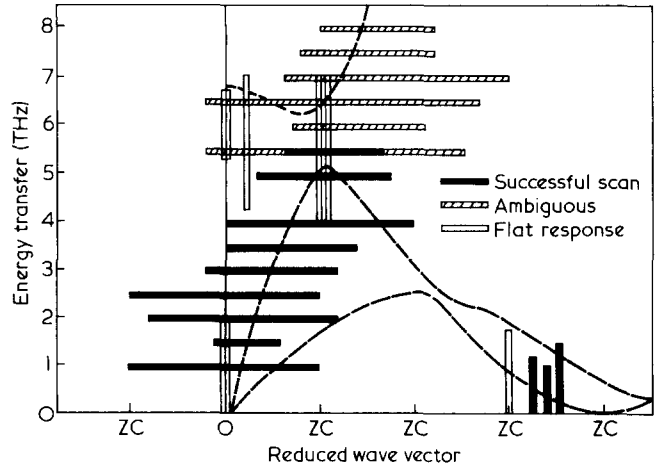

Figure 12 Range of phonon scans in the c^*–a^* plane of deutero-polyoxymethylene at 298K

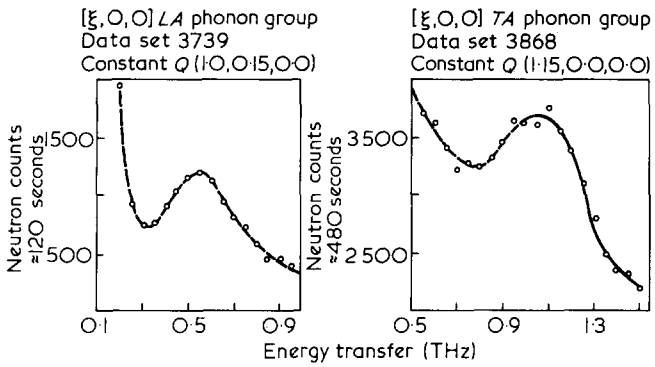

Figure 13 Typical phonons for the basal plane phonon branches in deutero-polyoxymethylene at 298K

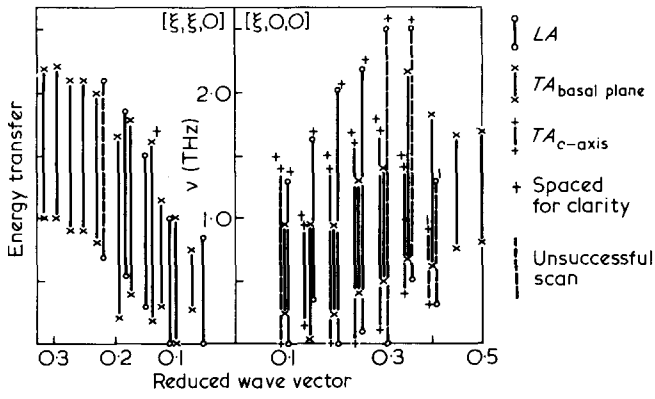

Figure 14 Summary of the scans made using IN8

the continuation of $LA(001)$ in the next Brillouin zone also gave ambiguous results.

Intensity from phonons was observed in several other scans but their identification either with particular branches in Zerbi's model, or with optical data, is indefinite and they remain unassigned. Several broad peaks, probably arising from incoherent scattering in regions of high densities of states, were observed. There were recurrent features at about 6 THz and 2.5 THz, the latter corresponding to the strongest singularity in the neutron time-of-flight spectrum of deutero-polyoxymethylene.

Phonons propagating in the basal plane (IN2, IN8). In the initial experiments using IN2, a third branch corresponding to $TA(1,0,0)$ was easily obtained. Its transverse nature was deduced from observation near (1,0,18), hence it is the TA mode polarized along the (0,0,1) direction. The phonon peaks from this branch were classical transverse acoustic peaks—intense and very narrow. Searches for the longitudinal and other transverse modes propagating and polarized in the basal plane were not successful. These modes were found, however, using IN8 in scans about the (1,0,0) point and the transverse mode $TA(1,0,0)$, previously observed, was confirmed. Transverse and longitudinal branches along the (1,1,0) direction were also observed.

The $TA(1,0,0)$ polarized along (0,0,1) was seen around (0,0,9) in constant Q scans. The TA (1,0,0) polarized in the basal plane was followed to 0.45 $\left(\frac{2\pi}{a}\right)$ but the intensity dropped markedly towards the zone boundary. The LA (1,0,0) was observed away from (1,0,0) to about 0.25 $\left(\frac{2\pi}{a}\right)$ where the intensity became weak. Typical phonons for two branches are shown in *Figure 13*. The (1,0,0) point was also used to observe $LA(110)$ and $TA(110)$ (polarized in the basal plane). The TA mode was strong and well resolved right out to the zone boundary but the longitudinal mode disappeared halfway to the Brillouin zone boundary. *Figure 14* summarizes the scans made using IN8.

Figure 15 shows all of the observed branches for both the c-axis and the basal plane.

DISCUSSION

The heat-treated deutero-polyoxymethylene 'crystal' used in the above experiments was macroscopically fibrous and gave both high and low angle neutron diffraction patterns. These were similar in general appearance to patterns from previous X-ray studies of γ-ray polymerized trioxane. We conclude, therefore, by analogy, that our crystal contains fibrils of approximately 200 Å diameter formed by contraction of the POM with respect to the trioxane crystal as the polymer forms. From high angle diffraction, the c-axis pole figure was determined and showed that chain alignment was better than 0.5°. Disorder between and within the fibrils is indicated respectively by the 4° width of equatorial reflections (e.g. (100)) for rocking about the c-axis and by the width of reflections along row lines of the helical diffraction pattern. The molecular disorder in the fibrils, as seen through the row line widths, is consistent with an effective short-range order of about 15 Å perpendicular to the c-axis. The corresponding measurement in the c direction from the layer line widths is limited by the machine resolution but we may set a lower limit of about 100 Å. We suspect that this intrinsic disorder is the major limitation for phonon dispersion curve measurements in this crystal. At the same time, since the crystal structure is incompletely determined, models of the dynamics cannot be made using the atom–atom potential method which requires atomic resolution. We were thus not able to compare the observed portions of the phonon dispersion curves with a three-dimensional model calculation. The agreement of the c-axis longitudinal mode with the isolated chain calculation is fairly good.

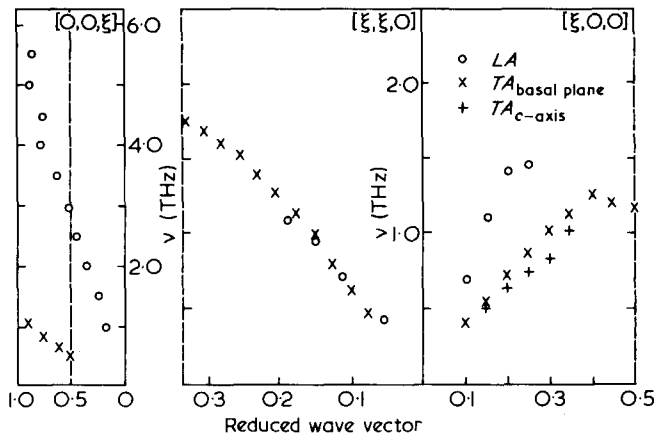

Figure 15 Measured phonon dispersion curves for deutero-polyoxymethylene at 298K

Table 3 Acoustic phonon velocities and corresponding stiffness constants for deutero-polyoxymethylene at 298K

Phonon branch	Velocity of sound (cm s^{-1})	Stiffness constant (dyne cm^{-2})
$LA(0,0,\xi)$	1.01×10^6	$C_{33} = 1.64 \times 10^{12}$
$TA(0,0,\xi)$	2.08×10^5	$C_{44}{}^{+} = 6.89 \times 10^{10}$
$LA(\xi,0,0)$	2.86×10^5	$C_{11} = 1.30 \times 10^{11}$
$TA(\xi,0,0)_{Basal}$*	1.45×10^5	$\frac{1}{2}(C_{11}-C_{12}) = 3.34 \times 10^{10}$
$TA(\xi,0,0)_{c\text{-axis}}$*	1.29×10^5	$C_{44} = 2.64 \times 10^{10}$
$LA(\xi,\xi,0)$	1.47×10^5	
$TA(\xi,\xi,0)_{Basal}$*	1.47×10^5	
		$C_{12} = 6.32 \times 10^{10}$

* Polarization

+ This value is obtained by extrapolation back into the first Brillouin from phonon groups observed in the second zone and a better value is obtained from the first zone phonon groups of $TA(\xi,0,0)_{c\text{-axis}}$

The immediate result of the neutron inelastic scattering measurement, therefore, is a determination of some of the elements of the stiffness matrix for POM from the low energy slopes of the dispersion curve. For trigonal crystals the stiffness matrix is

$$\begin{pmatrix} C_{11} & C_{12} & C_{13} & C_{14} & -C_{25} & 0 \\ C_{12} & C_{11} & C_{13} & -C_{14} & C_{25} & 0 \\ C_{13} & C_{13} & C_{33} & 0 & 0 & 0 \\ C_{14} & -C_{14} & 0 & C_{44} & 0 & -C_{25} \\ -C_{25} & C_{25} & 0 & 0 & C_{44} & C_{14} \\ 0 & 0 & 0 & -C_{25} & C_{14} & \frac{1}{2}(C_{11}-C_{12}) \end{pmatrix}$$

For hexagonal crystals, C_{13}, C_{25} and C_{14} are zero but C_{14} should be kept because of the chain stiffness. We adopt a model of hexagonal symmetry as a first approximation with the idea of showing how far is the departure from a hexagonal case.

From standard elasticity equations for the hexagonal case it is readily obtained that:

$$\rho V^2_{(001)_L} = C_{33}$$

$$\rho V^2_{(001)_T} = C_{44}$$

$$\rho V^2_{(100)_L} = C_{11}$$

$$\rho V^2_{(100)_{T_{(001)}}} = C_{44}$$

$$\rho V^2_{(100)_{T_{(010)}}} = \tfrac{1}{2}(C_{11}-C_{12})$$

Table 3 lists the elastic stiffnesses and sound velocities for deutero-polyoxymethylene at 298K. The elastic constants have been calculated assuming a crystalline density of 1.59 g cm^{-3}.

The elastic anisotropy of the polyoxymethylene crystal resulting from the high chain stiffness is apparent from *Table 3*. The chain stiffness approaches that of the uncoiled chain of polyethylene (3.58×10^{12} dyne cm^{-2}) and is near to that calculated by Asahina and Enomoto[25] using a Urey–Bradley force field. The chain stiffness is more than a factor of three times the value measured by Sakurada[2] using the X-ray method[2]. The elastic constant C_{11} in the basal plane is also nearly a factor of two times the 'modulus perpendicular to the chain' measured by the X-ray method[2]. There are no macroscopic or X-ray measurements with which to compare the shear moduli. Hexagonal symmetry requires that the velocities of $TA(00\xi)$ and $TA(\xi 00)$ should be the same; the observed inequality reflects on the degree of distortion to the trigonal and indicates that, in addition to the second transverse mode in the basal plane, measurements at 45° to the *c*-axis and *ab* planes will be needed to obtain the remaining elements of the stiffness matrix: C_{12}, C_{13}, C_{14}.

While the *LA* dispersion curves for *c*-axis polarized excitations shown in *Figure 13* agree quite well with the isolated chain calculations by Piseri and Zerbi[18] for hexagonal polyoxymethylene, the fit is rather poor for the transverse branch over the measured ranges. This result supports the conclusion found for polyethylene[7] that interchain forces make only a very small contribution to stiffness in the *LA* mode but significantly affect the *TA* excitations. The main object of future work on this crystal will be to model the interchain forces in the presence of disorder between the chains. For this, further studies of the disorder by high and low angle diffraction are planned.

REFERENCES

1 Sharples, A. Polymer Science (Ed. A. D. Jenkins), North Holland, Ch. 4, 1972
2 Holliday, L. and White, J. W. Proc. Macromol. Symp. I.U.P.A.C., Leiden, August 1970. *Pure Appl. Chem.* 1971, **26**, 545
3 Kambour, R. P. and Robertson, R. E. Polymer Science (Ed. A. D. Jenkins), North Holland, Ch. 11, p. 757, 1972
4 Sakurada, I., Ito, T. and Nakamae, K. *J. Polym. Sci.* 1966, **C15**, 75
5 Odajima, A. and Maeda, T. *J. Polym. Sci.* 1966, **C16**, 55
6 White, J. W. Polymer Science (Ed. A. D. Jenkins), North Holland, Ch. 27, 1972
7 Feldkamp, L. A. *et al.* in Inelastic Scattering of Neutrons, Proc. Symp. Copenhagen 1968. Vol. 2, I.A.E.A. Vienna, p. 159, 1969
8 La Garde, V. *et al. Disc. Faraday Soc.* 1969, **48**, 15
9 Piseri, L. *et al. J. Chem. Phys.* 1973, **58**, 158
10 Reynolds, P. A., Twistleton, J. F. and White, J. W. *Polymer* 1982, **23**, 578
11 Twisleton, J. F. and White, J. W. *Polymer* 1972, **13**, 40
12 Twisleton, J. F. and White, J. W. Neutron Inelastic Scattering, Proc. Symp. Grenoble, I.A.E.A. Vienna, p. 301, 1972
13 Uchida, T. and Tadokoro, H. *J. Polym. Sci. A2*, 1967, **5**, 63
14 Chatani, J. *et al. J. Macromol. Sci.-Phys.* 1968, **B2**, 567
15 Carazzolo, G. A. *J. Polym. Sci.* 1963, **A1**, 1573
16 Flory, P. J. and Mark, H. *Macromol. Chem.* 1964, **75**, 11
17 Gramlick, V. Paper PII64 in X-ray 76, Diffraction Meeting Oxford proceedings, p. 531, 1976
18 Piseri, L. and Zerbi, G. *J. Chem. Phys.* 1968, **48**, 3561
19 Cochran, W. *et al. Acta Cryst.* 1952, **5**, 581
20 Munoz, A. *et al.* I.U.P.A.C., International symposium on macromolecules, Leiden, Abstracts, Vol. II, p. 703, 1970
21 Colson, J. P. and Reneker, D. H. *J. Appl. Phys.* 1970, **41**, 4296
22 Reneker, D. H. and Colson, J. P. *Appl. Phys.* 1971, **42**, 4606
23 Groves, G. *et al.* Dept. of Metallurgy, Oxford University—private communication
24 Truell, R. *et al.* Ultrasonic Methods in Solid State Physics, Academic Press, London, 1969
25 Asahina, M. and Enomoto, S. *J. Polym. Sci.* 1962, **59**, 101